Journal of Solid State Chemistry 182 (2009) 43–48

Contents lists available at ScienceDirect

Journal of Solid State Chemistry

journal homepage: www.elsevier.com/locate/jssc

Synthesis, structure determination, and infrared spectroscopy of $(NpO_2)_2(SO_4)(H_2O)_4$: Prevalence of cation–cation interactions and cationic nets in neptunyl sulfate compounds

T.Z. Forbes, P.C. Burns *

Department of Civil Engineering and Geological Sciences, University of Notre Dame, 156 Fitzpatrick Hall, Notre Dame, IN 46556, USA

ARTICLE INFO

Article history:
Received 16 July 2008
Received in revised form
21 August 2008
Accepted 31 August 2008
Available online 8 October 2008

Keywords:
Actinide
Neptunium
Sulfate
Crystal structure
Single crystal X-ray diffraction

ABSTRACT

The compound $(NpO_2)_2(SO_4)(H_2O)_4$ was synthesized by evaporation of a Np^{5+} sulfate solution. The crystal structure was determined using single crystal X-ray diffraction and refined to an $R_1 = 0.0310$. $(NpO_2)_2(SO_4)(H_2O)_4$ crystallizes in triclinic space group $P\text{-}1$, $a = 8.1102(7)$ Å, $b = 8.7506(7)$ Å, $c = 16.234(1)$ Å, $\alpha = 90.242(2)^\circ$, $\beta = 92.855(2)^\circ$, $\gamma = 113.067(2)^\circ$, $V = 1058.3(2)$ Å^3, and $Z = 2$. The structure contains neptunyl pentagonal bipyramids that share vertices through cation–cation interactions to form a sheet or cationic net. The sheet is decorated on each side by vertex sharing with sulfate tetrahedra, and adjacent sheets are linked together through hydrogen bonding. A graphical representation of $(NpO_2)_2(SO_4)(H_2O)_4$ was constructed to facilitate the structural comparison to similar Np^{5+} compounds. The prevalence of the cationic nets in neptunyl sulfate compounds related to the overall stability of the structure is also discussed.

1. Introduction

The crystal chemistry of the early actinides has received increased attention over the past decade due to their rich structural diversity [1] as well as their importance in nuclear waste management [2–4], transport of radionuclides within the environment [5], and novel nanomaterials [6,7]. Hexavalent uranium compounds in particular have been intensely studied with the structures of over 360 compounds now known, 80 of which are mineral species [1]. Less is known about Np^{5+} compounds, although structural divergence from U^{6+} crystal chemistry has been observed [8–11].

Both U^{6+} and Np^{5+} cations occur in crystal structures as nearly linear dioxo cations that are further coordinated by four, five, or six ligands arranged at the equatorial vertices of square, pentagonal and hexagonal bipyramids [12]. The coordination polyhedra about the uranyl and neptunyl ions have very similar shapes and bond lengths, but the lower valence of the neptunyl ion stipulates different bonding requirements [2]. The axial oxygen atom on the uranyl ion is nearly satisfied by bonding to the U^{6+} cation alone; however, the neptunyl oxygen atom can form somewhat stronger bonds.

Bonding requirements for the O atom of the $(NpO_2)^+$ cation can be satisfied through interactions with other neptunyl polyhedra. Specifically the O atom of the linear $(NpO_2)^+$ cation can be an equatorial ligand of a neighboring $(NpO_2)^+$ cation. This type of bonding is historically referred to as a "cation–cation" interaction. First observed in solutions by Sullivan et al. in 1961 [13], these linkages are relatively common in Np^{5+} crystal chemistry, occurring in approximately half of the reported structures [14]. Cation–cation interactions are rare in U^{6+} crystal chemistry, as the O atom of the $(UO_2)^{2+}$ cation is generally satisfied and bonding between the uranyl polyhedra primarily occurs through the equatorial plane [1].

We have undertaken a detailed investigation of Np^{5+} crystal chemistry, to provide an increased understanding of Np^{5+} structural chemistry, as well as assisting in a fundamental understanding of Np^{5+} solution chemistry [4,8,9,14,15]. Here we present the synthesis, structure determination and infrared spectroscopy of the compound $(NpO_2)_2(SO_4)(H_2O)_4$ and discuss the prevalence of cation–cation interactions and cationic nets in the structures of neptunyl sulfate compounds.

2. Experimental methods

2.1. Crystal synthesis

The starting Np^{5+} material was recovered from previous experiments, purified through a cation-exchange column using Dowex-50-X8 resin, and dissolved in a 1 M HCl solution. A UV

* Corresponding author. Fax: +1 574 631 9236.
E-mail addresses: tziemann@nd.edu (T.Z. Forbes), pburns@nd.edu (P.C. Burns).

0022-4596/$ - see front matter © 2008 Elsevier Inc. All rights reserved.
doi:10.1016/j.jssc.2008.08.032

spectrum was collected for the final stock solution (98 mM) to ensure that the solution contained only pentavalent neptunium. *CAUTION*: *^{237}Np is a strong alpha emitter and represents a serious health risk. Such studies should only be performed using appropriate equipment and personnel for handling radioactive materials.* The sulfate source, $Zn(SO_4)(H_2O)$ (0.071 g), was loaded into a 7 mL Teflon cup with a screw top lid. A clear emerald green solution was formed with the addition of 0.50 mL of the Np^{5+} stock solution, and 0.50 mL of ultrapure water. The pH was then adjusted from 0.81 to 4.88 with the addition of 1.09 mL of 1.0 M NH_4OH. The Teflon cups were then closed tightly and placed into a 125 mL Teflon-lined Parr reaction vessel. Approximately 50 mL of ultrapure water (18 MΩ resistance) was added to provide counter pressure during heating. The reaction vessel was heated in a gravity convention oven at 150 °C for one week. Crystals did not form during the heat cycle, thus the solution was allowed to evaporate for promote crystal growth. After one week, green plates approximately 100 μm in length were recovered from the solution.

2.2. Structure solution and refinement

A single crystal of $(NpO_2)_2(SO_4)H_2O_4$ was isolated from the solution, mounted on a tapered glass fiber using epoxy, and placed on a Bruker PLATFORM three-circle X-ray diffractometer equipped with an APEX CCD detector. A sphere of three-dimensional data was collected at room temperature using monochromatic Mo*K*α radiation, frame widths of 0.3 in ω, and a count time per frame of 20 s. Unit cell parameters were refined by least-squares techniques using the Bruker SMART software [16] and the SAINT software [17] was used for data integration. A semi-empirical absorption correction was applied using the Bruker SADABS program, which lowered the R_{int} from 0.1302 to 0.0370. Selected data collection parameters and crystallographic data are provided in Table 1.

The structure was solved by direct methods and refined on the basis of F^2 for all unique data using the Bruker SHELXTL Version 5 system of programs [18]. Atomic scattering factors for each atom were taken from the International Tables for X-ray crystallography [19]. $(NpO_2)_2(SO_4)(H_2O)_4$ crystallizes in triclinic space group *P*-1. The Np and S cations were found using direct methods solutions, while the O atoms were located in the difference-Fourier maps following least-squares refinement of the partial-structure model. The final model includes anisotropic displacement parameters for all non-H atoms. H atom positions were refined with the soft constraint that O–H bonds be approximately 0.96 Å. The selected interatomic distances for $(NpO_2)_2(SO_4)(H_2O)_4$ are given in Table 2. Further details of the crystal structure determination can be obtained from the Fachinformationszentrum Karlsruhe, 76334 Eggenstein Leopoldshafen, Germany, (fax: 49 7247 808 666; e-mail: crystdata@fiz.karlsruhe.de) on quoting the depository number CSD 419688.

2.3. Infrared spectroscopy

An infrared spectrum of $(NpO_2)_2(SO_4)(H_2O)_4$ was collected on a single crystal of the material using a SensIR microspectrometer equipped with an diamond ATR objective. The spectrum was collected from 400 to 4000 cm^{-1} with a 100 μm beam aperture.

3. Results

3.1. Structural description

$(NpO_2)_2(SO_4)(H_2O)_4$ contains sheets of neptunyl polyhedra linked through cation–cation interactions and decorated by sulfate tetrahedra. There are four symmetrically independent Np^{5+} cations that are strongly bonded to two O atoms, resulting in a nearly linearly neptunyl cation, $(NpO_2)^+$. The bond lengths range from 1.833(3) to 1.846(3) Å for the Np–O_{Np} (O_{Np} = neptunyl oxygen) bond. The $(NpO_2)^+$ cation is further coordinated by five O atoms located at the equatorial vertices of a pentagonal bipyramid that is capped by the neptunyl ion O atoms. The Np^{5+}–O_{eq} (eq: equatorial) bonds range from 2.391(3) to 2.553(4) Å.

Table 1
Selected crystallographic parameters for $(NpO_2)_2(SO_4)(H_2O)_4$

Formula	$(NpO_2)_2(SO_4)(H_2O)_4$
Formula weight (g)	706.0
Temperature (K)	293(2)
Crystal system	Triclinic, *P*-1
a (Å)	8.1102(7)
b (Å)	8.7506(7)
c (Å)	16.234(1)
α (°)	90.242(2)
β (°)	92.855(2)
γ (°)	113.067(2)
Volume (Å^3)	1058.3(2)
Z	2
D_{calc} (g cm^{-3})	4.432
μ (mm^{-1})	19.777
F(000)	1224
Crystal size (mm)	0.12 × 0.11 × 0.05
θ range	2.51°–34.51°
Data collected	−12<h<12, −13<k<13, −25<l<25
Reflections collected/unique	21734/8590 [R_{int} = 0.0403]
Completeness to θ = 34.51	95.8%
Refinement method	Full-matrix least-squares on F^2
Data/restraints/parameters	8590/16/319
Goodness-of-fit on F^2	1.019
Final *R* indicies [$I>2\sigma(I)$]	R_1 = 0.0310, wR_2 = 0.0662
R indices (all data)	R_1 = 0.0426, wR_2 = 0.0705
Largest diff. peak and hole (Å^{-3})	1.937 and −1.757

Table 2
Selected interatomic distances (Å) for $(NpO_2)_2(SO_4)(H_2O)_4$

Np(1)–O(3)	1.833(3)	Np(4)–O(5)	1.839(3)
Np(1)–O(4)	1.836(4)	Np(4)–O(11)	1.846(3)
Np(1)–O(5)	2.401(3)	Np(4)–O(6)[d]	2.398(4)
Np(1)–O(9)[a]	2.416(3)	Np(4)–O(10)	2.410(4)
Np(1)–O(7)	2.448(4)	Np(4)–O(2)	2.418(4)
Np(1)–OW(1)	2.468(4)	Np(4)–OW(8)	2.481(4)
Np(1)–OW(2)	2.471(4)	Np(4)–OW(7)	2.545(4)
⟨Np(1)–O_{eq}⟩	2.441	⟨Np(4)–O_{eq}⟩	2.450
Np(2)–O(13)	1.837(3)	S(1)–O(15)[c]	1.462(4)
Np(2)–O(9)	1.840(3)	S(1)–O(10)	1.467(4)
Np(2)–O(4)	2.402(4)	S(1)–O(8)	1.481(4)
Np(2)–O(3)[b]	2.413(3)	S(1)–O(1)	1.487(4)
Np(2)–O(16)	2.442(4)	⟨S(1)–O⟩	1.474
Np(2)–OW(4)	2.499(4)		
Np(2)–OW(3)	2.553(4)	S(2)–O(16)[d]	1.469(4)
⟨Np(2)–O_{eq}⟩	2.462	S(2)–O(12)[a]	1.467(4)
		S(2)–O(7)	1.476(4)
Np(3)–O(2)	1.834(3)	S(2)–O(14)	1.481(4)
Np(3)–O(6)	1.838(3)	⟨S(2)–O⟩	1.473
Np(3)–O(13)	2.391(3)		
Np(3)–O(11)[c]	2.391(3)		
Np(3)–O(1)	2.454(4)		
Np(3)–OW(6)	2.490(4)		
Np(3)–OW(7)	2.494(4)		
⟨Np(3)–O_{eq}⟩	2.444		

Symmetry transformations used to generate equivalent atoms: a: −*x*+1, −*y*+2, −*z*+1; b: *x*+1, *y*, *z*; c: −*x*+1, −*y*+2, −*z*; d: *x*-1, *y*, *z*.

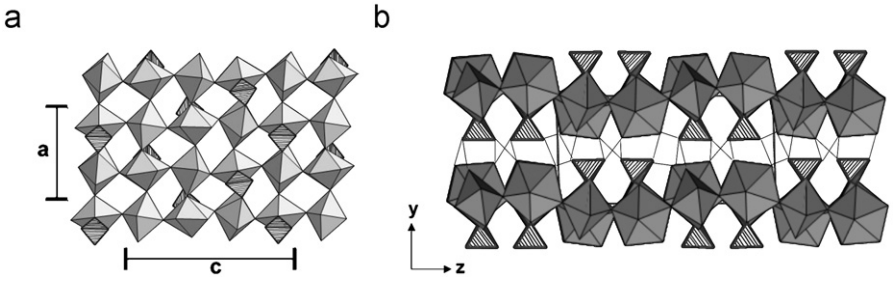

Fig. 1. (a) Polyhedral representation of the sheet in $(NpO_2)_2(SO_4)(H_2O)_4$ illustrating the cation–cation interactions between the neptunyl polyhedra to create sheets that are decorated by sulfate tetrahedra. (b) The sheets are held together by hydrogen bonding in the interlayers.

The neptunyl pentagonal bipyramids are linked together into a two-dimensional sheet by sharing of polyhedral vertices (Fig. 1a). The linkages between the neptunyl pentagonal bipyramids demand special attention, as all of the vertices are shared through cation–cation interactions. Each of the neptunyl oxygen atoms are linked to a neighboring neptunyl polyhedron through its equatorial vertex. These linkages create a two-dimensional sheet of cation–cation interactions that has been previously referred to as a "cationic net" that is comprised of $[(NpO_2)_2]^{2+}$ moieties [20].

Two symmetrically independent S atoms are located within the structure. The S atom bonds to four O atoms to create the SO_4^{2-} tetrahedra, with bond lengths ranging from 1.462(4) to 1.487(4) Å. The sulfate tetrahedra decorate both sides of the neptunyl pentagonal bipyramids to create a neutral net charge on the two-dimensional sheet (Fig. 1a). The sulfate tetrahedra share two of its vertices with two neighboring neptunyl pentagonal bipyramids, bridging the polyhedra in the [1 0 0] direction. The sulfate tetrahedra decorate the top of the sheet along chains of polyhedra that are two neptunyl pentagonal bipyramids wide (Fig. 1a). The sulfate tetrahedra then decorate the next two neptunyl polyhedra chains on the opposite side of the sheet. This pattern continues with two neptunyl sulfate chains on top of the sheet, followed by two at the bottom.

Each neptunyl pentagonal bipyramid contains H_2O groups at two of its equatorial vertices, pointing towards the interstitial space between the sheets (Fig. 1b). The bond distance between the H atom and its O acceptor ranges from 1.83 to 2.36 Å. A list of the O acceptors and H–O acceptor lengths for the H_2O groups is given in Table 3. The H_2O ligands link the neutral neptunyl sulfate sheets together through hydrogen bonds.

Table 3
The O acceptors and H–O acceptor lengths for the H_2O groups in $(NpO_2)_2(SO_4)(H_2O)_4$

H_2O group	H atom	O acceptor	O acceptor length
OW(1)	H(1)	O(8) on S(1) tetrahedron	1.92
	H(2)	O(14) on S(2) tetrahedron	1.83
OW(2)	H(3)	OW(3)	2.36
	H(4)	OW(12)	1.83
OW(3)	H(5)	O(8) on S(1) tetrahedron	1.99
	H(6)	O(7) on S(2) tetrahedron	2.06
OW(4)	H(7)	O(12) on S(2) tetrahedron	1.85
	H(8)	O(4) on Np(1) polyhedron	1.99
OW(5)	H(9)	O(14) on S(2) tetrahedron	2.05
	H(10)	O(8) on S(1) tetrahedron	1.84
OW(6)	H(11)	O(15) on S(1) tetrahedron	1.87
	H(12)	OW(7)	1.98
OW(7)	H(13)	O(1) on S(1) tetrahedron	2.00
	H(14)	O(14) on S(2) tetrahedron	2.06
OW(8)	H(15)	O(15) on S(1) tetrahedron	1.90
	H(16)	O(15) on S(1) tetrahedron	1.92

3.2. Infrared spectrum

The infrared spectrum of $(NpO_2)_2(SO_4)(H_2O)_4$ exhibits two major peaks at 626 and 1106 cm^{-1} that correspond to the ν_3 antisymmetric stretching vibration of the $(NpO_2)^+$ cation and the sulfate tetrahedron, respectively (Fig. 2) [20,21]. Generally the stretching vibration associated with $(NpO_2)^+$ is located at slightly higher wavenumbers (approximately 730 cm^{-1}). The presence of cation–cation interactions has been known to lower the vibrational frequency and also cause broadening of the $(NpO_2)^+$ peak [20]. With four symmetrically independent Np sites, peak splitting of the antisymmetric stretching vibration of $(NpO_2)^+$ is also expected. The stretching vibration associated with the neptunyl ion in $(NpO_2)_2(SO_4)(H_2O)_4$ does not exhibit peak broadening nor peak splitting. However, the symmetry about the four crystallographically independent Np sites is very similar, as all O_{Np} atoms are involved in cation–cation interactions. Thus the stretching frequency may be very similar for all sites, which could cause a single peak in the spectrum. The broad peak from 2370 to 3620 cm^{-1}, as well as the sharp peak at 1581 cm^{-1}, confirms the presence of H_2O within the neptunyl sulfate sheets [21].

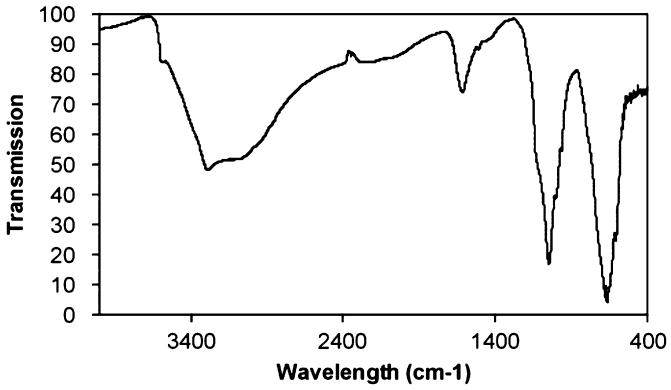

Fig. 2. The infrared spectrum of $(NpO_2)_2(SO_4)(H_2O)_4$.

4. Discussion

Graphical (or nodal) representations of structures have been utilized as an important technique to compare structural connectivities between diverse groups of compounds [22]. This approach has been used extensively for inorganic compound

including zeolites [23], aluminophosphates [24,25], borates [26], and uranyl oxysalts [1]. Recently, Forbes and Burns [14] suggested a graphical representation for Np^{5+} compounds, with black nodes representing Np^{5+} polyhedra and white nodes representing polyhedra of other higher valence cations such as sulfur. Connections between the nodes are represented by solid black lines, with a single line between two nodes representing vertex sharing between two polyhedra. Similarly, two lines indicate sharing of edges and three lines correspond to face sharing between the polyhedra. Cation–cation interactions are very common in Np^{5+} compounds, thus requiring additional attention in the graphical representation. Forbes and Burns [14] suggested the use of a single black link with an arrow pointing away from the donor oxygen on the neptunyl ion and towards the acceptor oxygen on the neighboring polyhedron as a way of distinguishing these linkages.

Following these guidelines, a graphical representation of the sheet in $(NpO_2)_2(SO_4)(H_2O)_4$ has been constructed (Fig. 3a). Each black node is linked to four other black nodes by single lines, with arrows designating the cation–cation interactions between the neptunyl polyhedra. Two arrows point towards the black node and two point away, indicating that all neptunyl oxygen atoms are involved in cation–cation interactions. White nodes symbolizing the bridging sulfate tetrahedra are connected to two black nodes through single black lines.

Graph theory can be extended to represent a hierarchy of structural units that correspond to the polymerization of higher-valence coordination polyhedra [22]. Such structural hierarchies organize complex structures into a cohesive system that facilitates recognition of structural trends. Graphical representations have been used extensively for uranyl molybdate compounds and showed that the resulting diagrams are mostly derived from a single parent graph by the simple deletion of nodes and connectors.

By constructing graphical representation of other Np^{5+} compounds, structural trends become apparent. A series of neptunyl sulfate compounds with the composition $(NpO_2)_2(SO_4)(H_2O)_n$ ($n = 1$, 2, and 6) have been synthesized by varying the reaction temperature (400 °C for $n = 1$, 200 °C for $n = 2$, and 25 °C for $n = 6$) [27] and their structures determined [28–30]. All three compounds contain neptunyl pentagonal bipyramids linked through cation–cation interactions. However $(NpO_2)_2(SO_4)(H_2O)$ does not form a cationic net. The framework of $(NpO_2)_2(SO_4)(H_2O)$ contains a dense cationic system of neptunyl polyhedra linked together by cation–cation interactions and vertex sharing with the sulfate tetrahedra (Fig. 3b) [28]. One of the Np polyhedra in this structure contains an unusual coordination geometry, as it shares an edge with a sulfate tetrahedron perpendicular to the equatorial edge of the neptunyl pentagonal bipyramid. The coordination number about the Np^{5+} cation is eight, with two axial bond lengths of approximately 1.874 Å, and six additional bonds ranging from 2.352 to 2.770 Å. However, the coordination polyhedron is no longer a hexagonal bipyramid.

The cationic net observed in $(NpO_2)_2(SO_4)(H_2O)_4$ is also found in $(NpO_2)_2(SO_4)(H_2O)_2$. However, the sheets in $(NpO_2)_2(SO_4)(H_2O)_2$ are further linked into a three-dimensional framework through vertex sharing between the sulfate tetrahedra and neptunyl pentagonal bipyramds (Fig. 3c) [29]. The neptunyl sulfate linkages within $(NpO_2)_2(SO_4)(H_2O)_6$ are also identical to $(NpO_2)(SO_4)(H_2O)_4$, but the additional H_2O groups terminate the sheet into a chain that is two neptunyl polyhedra wide (Fig. 3d) [30].

The structure of $NpO_2Cl(H_2O)$ also contains a cationic net of neptunyl polyhedra that is identical to that observed in $(NpO_2)_2(SO_4)(H_2O)_4$ [31]. This structure contains a Cl atom at one of the equatorial vertices on the neptunyl pentagonal bipyramids to create a neutral sheet. Several other Np^{5+} compounds also contain cationic nets connected into a three-dimensional framework,

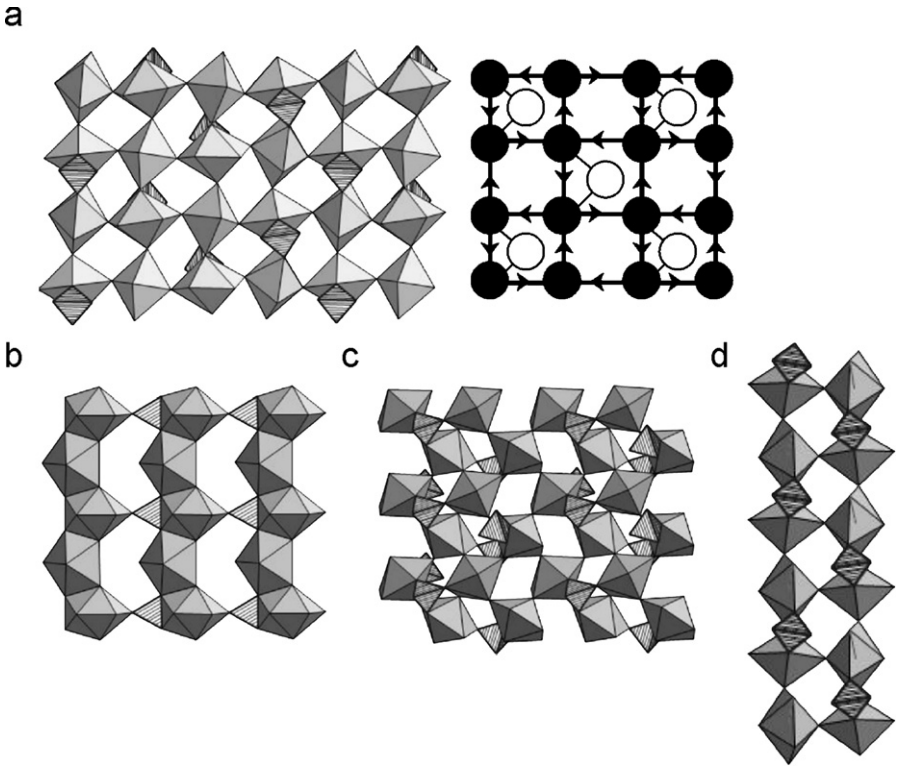

Fig. 3. (a) Graphical representation of $(NpO_2)_2(SO_4)(H_2O)_4$ with the black nodes depicting the Np^{5+} polyhedra and the white nodes representing the $(SO_4)^{2-}$ tetrahedra. The cation–cation interactions are displayed using arrows pointing from the neptunyl donor oxygen atom to the neptunyl acceptor. Additional structures with cationic nets from the neptunyl sulfate series (b) $(NpO_2)_2(SO_4)(H_2O)$ [28], (c) $(NpO_2)_2(SO_4)(H_2O)_2$ [29], and (d) $(NpO_2)_2(SO_4)(H_2O)_6$ [30].

including $(NpO_2)(IO_3)$ [32], β-$Ag(NpO_2)(SeO_3)$ [32], $Na(NpO_2)(SO_4)(H_2O)$ [9], and $NaK_3(NpO_2)_4(SO_4)(H_2O)_2$ [9]. The simplest frameworks include the structures of $(NpO_2)(IO_3)$ and β-$Ag(NpO_2)(SeO_3)$. Neptunyl pentagonal bipyramids are linked through cation–cation interactions to create a cationic net that is connected into a framework structure through vertex sharing with the $(IO_3)^-$, $(SeO_3)^{2-}$ or $(SO_4)^{2-}$ polyhedra. $NaK_3(NpO_2)_4(SO_4)_4(H_2O)_2$ and $Na(NpO_2)(SO_4)H_2O$ contain chains that are four neptunyl pentagonal bipyramids wide and that are connected through cation–cation interactions. These chains contain the building blocks for the cationic nets and are terminated into chains through vertex sharing with sulfate tetrahedra. The sulfate tetrahedra also connect the neptunyl pentagonal bipyramid chains together into a three dimensional framework by sharing of the tetrahedral vertices with bipyramids of adjacent chains.

The propensity of neptunyl sulfates to form cationic nets through cation–cation interactions is unusual. Other neptunyl compounds containing $(X^{6+}O)_4^{2-}$ polyhedra, such as molybdates and chromates, form sheets and frameworks, but do not contain dense networks of neptunyl polyhedra bonded through cation–cation interactions [11,33–35]. Instead, the polyhedra in these compounds are generally linked through the sharing of vertices between the $(X^{6+}O)_4^{2-}$ tetrahedra and the neptunyl polyhedra. Cation–cation interactions still occur, but are limited to isolated linkages between two neptunyl polyhedra or connect the two-dimensional sheets into a framework structure.

Although studies have shown many structural differences between Np^{5+} and U^{6+} compounds [9], the wealth of crystallographic information for U^{6+} may offer some clues for the predisposition of cationic nets in Np^{5+} sulfate structures. A review of the structural chemistry of U^{6+} sulfate compounds reveals that only two structures contain direct linkages between uranyl polyhedra. Instead, most connections within these compounds occur through the sharing of the $(SO_4)^{2-}$ tetrahedral vertices with the uranyl polyhedra [36]. Up to four of the $(SO_4)^{2-}$ tetrahedra are shared between the uranyl polyhedra although the U–O–S bond angles must be distorted to accommodate the four linkages.

Monodentate linkages between the uranyl ion and sulfate tetrahedra have also been observed in aqueous solutions. High energy X-ray scattering studies indicated that the U–O–S bond angle of the uranyl sulfate complex appears nearly constant in solution, prompting Newufeind et al. 2004 [37] to conclude that an U–O–S angle of 143° is an intrinsic property of the uranyl sulfate bond. Many solid state structures from the literature appear to support this conclusion, except when four of the sulfate tetrahedra vertices are shared [37]. A study by Forbes et al. 2007 [36] found that the average U–O–S bond decreased to 128.2° when all four sulfate vertices were shared with uranyl polyhedra. They concluded that the deviations of the U–O–S bond angle from the average value, especially where all tetrahedral vertices are shared, is most likely caused by steric constraints of the structure. The compound may tolerate the distortions of the U–O–S angle if the energetics of the sheet is favored over the energetics of the local environment.

Several uranyl compounds contain $(SO_4)^{-2}$ tetrahedra that share four vertices, including the uranyl sulfate minerals zippeite and uranopilite [38,39]. These uranyl sulfate minerals are widespread and have existed for thousands of years within geologic systems [40]. In contrast, a majority of the compounds with one, two, or three vertex linkages are synthetic, and are not known to form or endure under natural conditions. Thus, the distortion in the U–O–S angle may not affect the overall stability of the structure and additional bonding to all four O atoms on the vertices of the tetrahedra may in fact increase the stability of the compound.

The presence of the cationic nets within the neptunyl sulfate structures may be more favorable for sharing multiple vertices of the sulfate tetrahedra that may contribute to the structural stability. The presence of cation–cation interactions within the cationic nets promotes different orientations of the neptunyl polyhedra, which may create more favorable angles for sharing of tetrahedral vertices (Fig. 4). Table 4 summarizes the average bond angle for uranyl sulfate compounds with two or four linkages to sulfate tetrahedra and compares them to neptunyl sulfate compounds with similar numbers of linkages that contain cationic nets. The Np–O–S bond angle in solution has not been measured, but if we assume it is similar to the U–O–S angle (143°), then the distortion of the Np–O–S bond angle is less with four shared sulfate vertices when cation–cation interactions are present in the structure. Less distortion of the Np–O–S bond angle may be more favorable for the local energetics and may lead to more stability of the overall structure.

Cation–cation interactions are rare in U^{6+} compounds, but do occur in the structures of α-$(UO_2)(SeO_4)$ [41], β-$(UO_2)(SO_4)$ [41], and $(UO_2)(MoO_4)$ [42]. These compounds are isostructural and contain chains of cation–cation interaction that are two polyhedra wide and are similar to the chains found in $Na(NpO_2)(SO_4)(H_2O)$ and $NaK_3(NpO_2)_4(SO_4)_4(H_2O)_2$ [9]. The chains are linked into a framework through sharing of four vertices to the $(X^{6+}O)_4$ tetrahedra. The presence of cation–cation interactions in these uranyl structures emphasizes the possible importance of cation–cation interactions in the stability of both uranyl and neptunyl sulfates. Further studies are needed to explore the role that cation–cation interactions play in the stability of actinyl structures.

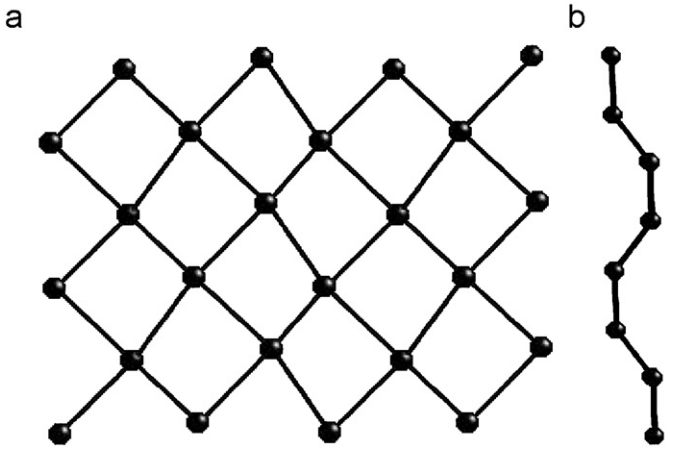

Fig. 4. (a) The cationic net found in $(NpO_2)_2(SO_4)(H_2O)_4$ can be represented by showing connectivities between the neptunyl polyhedra (represented as black spheres). (b) When the cationic net is rotated 90°, the curvature of the sheet becomes apparent.

Table 4
A comparison of the number of sulfate tetrahedra vertices shared to neighboring actinyl polyhedra related to the bond angle for uranyl and neptunyl sulfates

# of shared vertices	Average	Range	Between 130° and 150°	References
U no CCI				
2	141.2	123.6–160.0	12 out of 13	[43–53]
4	128.2	119.8–140.5	1 out of 11	[38,39,54]
Np with CCI				
2	140.4	125.3–156.6	7 out of 10	[9,30]
4	136.5	126.6–157.6	7 out of 13	[9,28,29]

All of the neptunyl compounds listed contain cationic nets that are linked through cation–cation interactions.

Acknowledgments

We thank Dr. L. Soderholm and Dr. S. Skanthakumar at Argonne National Laboratory for assistance. This research was funded by the National Science Foundation Environmental Molecular Science Institute at the University of Notre Dame (EAR02-21966).

References

[1] P.C. Burns, Can. Mineral. 43 (2005) 1839–1894.
[2] P.C. Burns, R.C. Ewing, M.L. J Miller, J. Nucl. Mater. 245 (1997) 1–9.
[3] P.C. Burns, K.M. Deely, S. Skanthakumar, Radiochim. Acta 92 (2004) 151–159.
[4] T.Z. Forbes, P.C. Burns, Am. Mineral. 91 (2006) 1089–1093.
[5] J. Brugger, P.C. Burns, N. Meisser, Am. Mineral. 88 (2003) 676–685.
[6] P.C. Burns, K.-A. Kubatko, G. Sigmon, B.J. Fryer, J.E. Gagnon, M.R. Antonio, Angew. Chem. Int. Ed. 44 (2005) 2135–2139.
[7] S.V. Krivovichev, V. Kahlenberg, I.G. Tananaev, R. Kaindl, E. Mersdorf, B.F.J. Myasoedov, Am. Chem. Soc. 127 (2005) 1072–1073.
[8] T.Z. Forbes, P.C.J. Burns, Solid State Chem. 178 (2005) 3445–3452.
[9] T.Z. Forbes, P.C. Burns, L. Soderholm, S. Skanthakumar, Chem. Mater. 18 (2006) 1643–1649.
[10] M.S. Grigor'ev, I.A. Charushnikova, N.N. Krot, A.I. Yanovskii, Y.T.Z. Struchkov, Neorg. Khim. 39 (1994) 179–183.
[11] M.S. Grigor'ev, T.E. Plotnikova, N.A. Baturin, N.A. Budantseva, A.M. Fedoseev, Radiochemistry 37 (1995) 102–105.
[12] P.C. Burns, R.C. Ewing, F.C. Hawthorne, Can. Mineral. 35 (1997) 1551–1570.
[13] J.C. Sullivan, J.C. Hindman, A.J.J. Zielen, Am. Chem. Soc. 83 (1961) 3373–3378.
[14] T.Z. Forbes, P.C.J. Burns, Solid State Chem. 180 (2007) 115–121.
[15] T.Z. Forbes, P.C. Burns, L. Soderholm, S.J. Skanthakumar, Am. Chem. Soc. 129 (2007) 2760–2761.
[16] SMART Software, Bruker Analytical X-ray Systems, Madison, WI, USA, 1998.
[17] SAINT Software, Bruker Analytical X-ray Systems, Madison, WI, USA, 1998.
[18] SHELXTL, Bruker Analytical X-ray Systems, Madison, WI, USA, 1998.
[19] J.A. Ibers, W.A. Hamilton, (Eds.), International Tables for X-ray Crystallography, Kynoch Press, Birmingham, UK, 1974, vol. IV.
[20] N.N. Krot, M.S. Grigoriev, Russ. Chem. Rev. 73 (2004) 89–100.
[21] J. Cejka, in: P.C. Burns, R. Finch (Eds.), Uranium: Mineralogy, Geochemistry and the Environment, vol. 38, Mineralogical Society of America, Washington, DC, USA, 1999, pp. 521–622.
[22] S.V. Krivovichev, Crystallogr. Rev. 10 (2004) 185–232.
[23] J.V. Smith, Chem. Rev. 88 (1988) 149–182.
[24] J. Yu, K. Sugiyama, K. Hiraga, N. Togashi, O. Terasaki, Y. Tanaka, S. Nakata, S. Qiu, R. Xu, Chem. Mater. 10 (1998) 3636–3642.
[25] J. Yu, R. Xu, Acc. Chem. Res. 36 (2003) 481–490.
[26] P.C. Burns, J.D. Grice, F.C. Hawthorne, Can. Mineral. 33 (1995) 1131–1151.
[27] N.A. Budantseva, A.M. Fedoseev, M.S. Grigor'ev, T.I. Potemkina, T.V. Afanas'eva, N.N. Krot, Radiokhimiya 30 (1988) 607–610.
[28] M.S. Grigor'ev, N.A. Baturin, N.A. Budantseva, A.M. Fedoseev, Radiokhimiya 35 (1993) 29–38.
[29] M.S. Grigor'ev, A.I. Yanovskii, A.M. Fedoseev, N.A. Budantseva, Y.T. Struchkov, N.N. Krot, V.I. Spitsyn, Dokl. Akad. Nauk SSSR 300 (1988) 618–622.
[30] I.A. Charushnikova, N.N. Krot, I.N. Polyakova, Crystallogr. Rep. 5 (2006) 201–204.
[31] M.S. Grigor'ev, A.A. Bessonov, N.N. Krot, A.I. Yanovskii, Y.T. Struchkov, Radiokhimiya 35 (1993) 17–23.
[32] T. Albrecht-Schmitt, P.M. Almond, R. Sykora, Inorg. Chem. 42 (2003) 3788–3795.
[33] M.S. Grigor'ev, N.A. Baturin, A.M. Fedoseev, N.A. Budantseva, Radiokhimiya 33 (1991) 53–63.
[34] M.S. Grigor'ev, A.M. Fedoseev, N.A. Budantseva, M.Y. Antipin, Radiochemistry 47 (2005) 545–548.
[35] M.S. Grigor'ev, I.A. Charushnikova, A.I. Yanovskii, Y.T. Struchkov, Radiokhimiya 34 (1992) 7–12.
[36] T.Z. Forbes, V. Goss, M. Jain, P.C. Burns, Inorg. Chem. 46 (2007) 7163–7168.
[37] J. Neuefeind, S. Skanthakumar, L. Soderholm, Inorg. Chem. 43 (2004) 2422–2426.
[38] P.C. Burns, K.M. Deely, L.A. Hayden, Can. Mineral. 41 (2003) 687–706.
[39] P.C. Burns, Can. Mineral. 39 (2001) 1139–1146.
[40] R. Finch, T. Murakami, in: P.C. Burns, R. Finch (Eds.), Uranium: Mineralogy, Geochemistry and the Environment, vol. 38, Mineralogical Society of America, 1999, pp. 91–180.
[41] N.P. Brandenburg, B.O. Loopstra, Acta Cryst. B 34 (1978) 3734–3736.
[42] V.N. Serezhkin, V.A. Efremov, V.K. Trunov, Kristallografiya 25 (1980) 861–865.
[43] L. Niinisto, J. Toivonen, J. Valkonen, Acta Chem. Scand. A 32 (1978) 647–665.
[44] L. Niinisto, J. Toivonen, J. Valkonen, Acta Chem. Scand. A 33 (1979) 621–624.
[45] A. Zalkin, H. Ruben, D.H. Templeton, Inorg. Chem. 17 (1978) 3701, 3701.
[46] Y.N. Mikhailov, Y.E. Gorbunova, E.V. Mit'kovskaya, L.B. Serezhkina, V.N. Serezhkin, Radiochemistry 44 (2002) 315–318.
[47] Y.N. Mikhailov, L.A. Kokh, V.G. Kuznetsov, T.G. Grevtseva, S.K. Sokol, G.V. Ellert, Koord. Khim. 3 (1977) 508–513.
[48] N.W. Alcock, M.M. Roberts, M.C. Chakravorti, Acta Cryst. B 36 (1980) 687–690.
[49] H. Ruben, B. Spencer, D.H. Templeton, Inorg. Chem. 19 (1980) 776–777.
[50] V.N. Serezhkin, M.A. Soldatkina, V.A.Z. Efremov, Strukt. Khim. 22 (1981) 174–177.
[51] R.F. Baggio, M.A.R. de Benyacar, B.O. Perazzo, P.K. de Perazzo, Acta Cryst. B 33 (1977) 3495–3499.
[52] V.V. Tabachenko, V.N. Serezhkin, L.B. Serezhkina, L.M. Kovba, Koord. Khim. 5 (1979) 1563–1568.
[53] N.W. Alcock, M.M. Roberts, Acta Cryst. B 38 (1982) 1805–1806.
[54] V.I. Spitsyn, L.M. Kovba, V.V. Tabachenko, N.V. Tabachenko, Y.N. Mikhailov, Izv. Akad. Nauk SSSR Khim. 4 (1982) 807–812.